

Determination of the Fermi Level Position for Neutron Irradiated High Resistivity Silicon Detectors and Materials Using the Transient Charge Technique(TChT)*

V. Eremin⁺ and Z. Li
Brookhaven National Laboratory
Upton, NY 11973, USA

+ : Permanent address: A.F. Ioffe Physico-Technical Institute of Academy of Sciences of Russia
St. Petersburg, Russia

Abstract

The transient charge technique (TChT) has been used in this work to study the electrical properties in both space charge region (SCR) and electrical neutral bulk (ENB) of neutron irradiated high resistivity (4-6 kΩ-cm) silicon particle detectors. Detectors irradiated to various neutron fluences were measured by TChT at various biases and temperatures from 110 K to 300 K. The Fermi level, obtained from the Arrhenius plot of the time constant of the ohmic relaxation component of the charge shape, has been found to stabilize around $E_c - 0.47$ to 0.50 eV at high fluences ($\Phi_n > 10^{13}$ n/cm²).

I. INTRODUCTION

Recently, much of the interest on the neutron radiation effects on high resistivity p⁺/n junction detectors has been concentrated on the high fluence ($\Phi_n > 10^{13}$ n/cm²) neutron induced changes of detector and material electrical properties (such as the detector leakage current, charge collection efficiency, full depletion voltage, etc.), in the wake of the anticipated high radiation environment (10^{14} n/cm² in ten years) in the newly proposed Large Hadron Collider.

The effective concentration of ionized space charges (sometimes also called : effective impurity concentration) N_{eff} in the space charge region (SCR), which determines the detector full depletion voltage V_d , as a function of neutron fluence has been mainly studied by the capacitance-voltage (C-V) technique[1-5], although there are some recent attempts using the transient current techniques (TCT), such as alpha[6] and laser [7] induced current shapes, to obtain V_d and N_{eff} . The C-V technique becomes less reliable at high neutron fluences due to high leakage current and frequency dependence[2]. The capacitance frequency dependence problem would make the traditional high frequency ($f > 100$ kHz) measurements impossible since they become insensitive to the detector bias (or the width of SCR). On the other hand, due to high leakage current after high fluence neutron radiation, the conductance has been observed to contribute

significantly to the low frequency capacitance measurements[3].

The material properties, or the electrical neutral bulk (ENB) properties, have been studied by entirely different techniques such as the four-point probe approach[8], the resistor structure approach[9], and the Hall effect approach[10-11]. All these approaches, however, are highly limited by the surface conditions and by the contact problems (ohmic contacts required).

In this paper, we will present the data of detector SCR properties such as N_{eff} , and ENB properties such as the position of the Fermi level as a function of neutron fluence using the transient charge technique (TChT). The main topic of this paper is to demonstrate the applicability of the TCT/TChT techniques to the systematic study of the electrical properties of irradiated silicon detectors in both SCR and ENB conditions. The details of experimental comparisons of N_{eff} obtained by the traditional C-V method and by the TCT/TChT techniques have been submitted elsewhere for publication[12].

II. EXPERIMENTAL

The block diagram of the laser TCT/TChT set-up at Brookhaven National Laboratory (BNL), designed at Physico-Technical Institute (PTI) and improved at BNL under the current PTI-BNL collaboration, is shown in Fig. 1. The sample was assembled on the copper table with heater and temperature control thermocouple, and the whole assembly was put inside a metal chamber. The chamber was covered by the glass bell protecting the chamber from a direct contact with liquid nitrogen surrounding it. The sample was AC coupled with the high frequency oscilloscope TDS-445 (Textronix) by a thin coaxial cable. Non equilibrium carriers were generated by a GaAs laser with a wave length of $\sim 0.8\mu$ m and a light pulse duration of ~ 1 ns. The diameter of the laser illumination spot on the detector was ~ 2 mm. The laser was pumped by nanosecond current pulses from a pulse generator through a current amplifier.

To shift the response pulse in time with respect to the triggering of the oscilloscope and to decrease the ripples induced by current pulse pumping, an optical delay line has

been used. As the optical fiber used in the existing set-up showed a strong dependence of transmission efficiency on temperature in the region below 230 K, the part of the optical fiber which might be cooled inside the cryostat was surrounded by a temperature controlled heater. This allowed the laser pulse energy deposited on the sample to be maintained to within an accuracy better than 1% at temperatures ranging from RT to 100 K. This set-up allows one to analyze detector waveforms of current pulses with amplitudes as small as ~ 1 mV, that corresponds to the generation of about 2×10^6 electron-hole pairs.

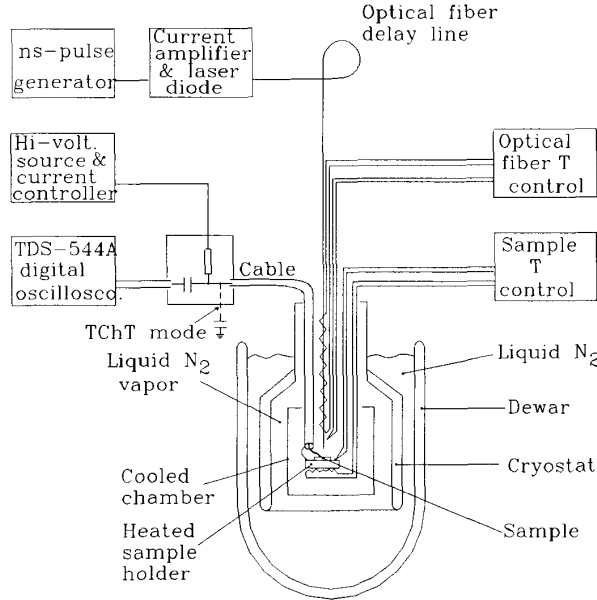


Fig. 1 Schematic of the TCT/TChT set-up at BNL.
Note for the TChT mode, an additional integral capacitor is needed.

III RESULTS AND DISCUSSIONS

An example of the laser induced current shape is shown in Fig. 2 for a non-irradiated detector. The detector was biased in a partially depleted mode and the laser illumination was on the p^+ side for which the current shape was mainly electron induced current. The main part of the theory which describes the shape of current and charge pulses induced by laser generated charges in the silicon detectors has been published in ref. [12-14].

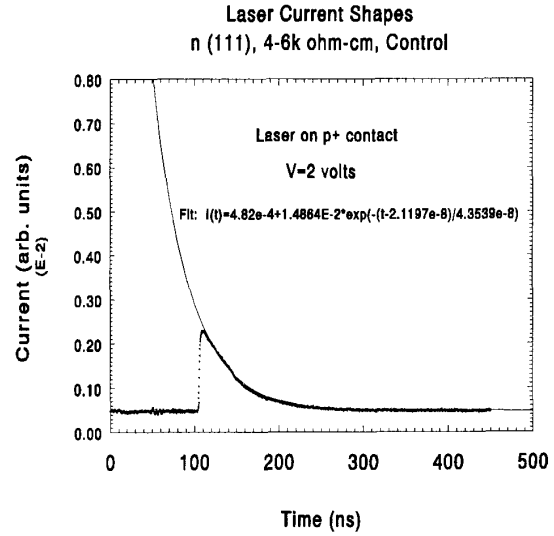


Fig. 2 Laser induced current shape for a non-irradiated detector ($\Phi_n = 0.0$ n/cm²). The laser illumination was on the p^+ side of the detector. Solid line is the fitting of the decay.

The general equation for the current pulse, taking into account the drift of generated charges in the SCR (drift current) and the relaxation of these charges in the ENB (ohmic current), is:

$$i(t) = \epsilon \epsilon_0 \frac{\partial E_b}{\partial t} + e \mu m E_b = \frac{Q_0 \mu E_0}{d} \left(\frac{1}{\tau_1} - \frac{1}{\tau_2} \right) \left[\frac{1}{\tau_2} \left(\frac{d}{W} - 1 \right) e^{-t/\tau_2} - \left(\frac{d}{W \tau_2} - \frac{1}{\tau_1} \right) e^{-t/\tau_1} \right] \quad (1)$$

where μ is the carrier mobility, E_0 is defined as, τ_1 and τ_2 are time constants defined as:

$$\begin{cases} \tau_1 = \frac{\epsilon \epsilon_0}{\mu e N_{eff}} = \tau_m^{SCR} \\ \tau_2 = \frac{\epsilon \epsilon_0}{\mu e n \text{ (or } p)} \cdot \frac{d}{W} = \tau_m^{ENB} \cdot \frac{d}{W} \end{cases} \quad (2)$$

Here the subscript m is used to denote the Maxwell relaxation time constant ($\tau = \epsilon \epsilon_0 \rho$) (which determines the kinetics of the transition of semiconductors from a non equilibrium free carrier distribution to the steady-state condition.), d is the detector thickness, n and p the free carrier concentrations for electrons and holes, respectively, and w the depletion width:

$$w = \sqrt{\frac{2\epsilon\epsilon_0 V}{eN_{eff}}} \quad (3)$$

where V is the reverse bias voltage.

For a non-irradiated detector:

$$\tau_m^{SCR} = \tau_m^{ENB} \quad (\text{no deep levels}) \quad (4)$$

and the current shape follows the exponential decay

e^{-t/τ_2} . The time constant for a non-irradiated detector is therefore dependent on both V and N_{eff} :

$$\tau_2 = \frac{d}{\mu} \cdot \sqrt{\frac{\epsilon\epsilon_0}{2eN_{eff}}} \cdot \frac{1}{\sqrt{V}} \quad (5)$$

Fig.3 shows $1/\tau^2$ for a non-irradiated detector as a function of the detector bias V . A clear linear dependence gives a N_{eff} of about 7.3×10^{11} atoms/cm³, very close to the value of 7.0×10^{11} atoms/cm³ obtained by us using the C-V method.

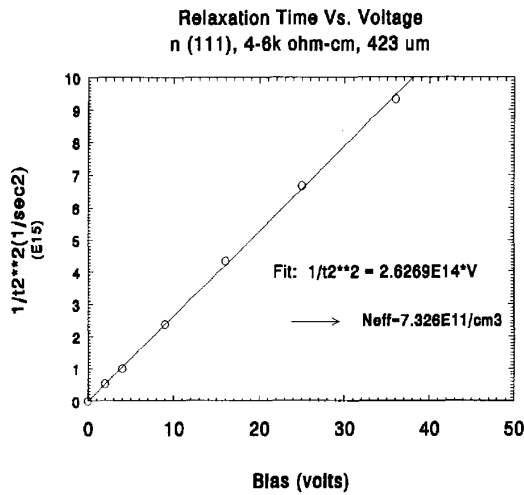


Fig. 3 The time constant τ obtained from fitting the exponential decay of the current shape of a non-irradiated detector as a function of the detector bias.

The charge shapes for an irradiated ($\Phi_n > 10^{13}$ n/cm²) detector at various biases at room temperature (RT) are shown in Fig. 4. We note here that the SCR of this detector has been converted to "p" type due to the creation of large amounts of ionized neutron induced acceptor defects. In other words, the sign of N_{eff} has changed from positive to negative and the junction has switched from the p⁺ side to the n⁺ side. We must emphasize here that N_{eff} is a measure of the net ionized space charges which include ionized impurities and charged defects created by neutrons and is therefore strictly a parameter for the SCR. The resistivity however, which is a measure of the free carrier concentration (n and p) and mobilities, is strictly a parameter for the ENB and it is entirely unrelated to N_{eff} for irradiated detectors (or $N_{eff} \neq n$ or p) [9]. It is clear that there are two components in the charge shape: a fast one that is associated with the drift current in the SCR (with a time constant τ_1) and a slow one for which the time constant τ_2 is related to the Maxwell relaxation time constant τ_m through eq. (4).

The total charge pulse can therefore be written as:

$$Q(t) = Q_{dr}^{SCR}(t) + Q_{\Omega}^{ENB}(t) \quad (6)$$

where the drift component is:

$$Q_{dr}^{SCR}(t) = Q_0 \frac{W}{d} (1 - e^{-t/\tau_1}) \equiv A_{dr} (1 - e^{-t/\tau_1}) \quad (7)$$

where A_{dr} is the charge amplitude for the drift component.

The ohmic component is:

$$Q_{\Omega}^{ENB}(t) = \frac{Q_0 \mu E_0}{d} \frac{\tau_1}{\tau_2 - \tau_1} \left(\frac{d}{W} - 1 \right) \cdot \left[\tau_2 (1 - e^{-t/\tau_2}) - \tau_1 (1 - e^{-t/\tau_1}) \right] \quad (8)$$

When $\tau_m^{SCR} \ll \tau_m^{ENB}$, $Q_{\Omega}^{ENB}(t)$ can be simplified as the following:

$$Q_{\Omega}^{ENB}(t) \approx Q_0 \left(1 - \frac{W}{d} \right) (1 - e^{-t/\tau_2}) \quad (9)$$

It follows from eq. (6) and (3) that the amplitude of the fast component (the drift component) A_{dr} of the charge shape increases with the bias V for less than full depletion ($V < V_d$), and saturates at the full depletion. In fact, A_{dr} is proportional to $V^{1/2}$ when $V < V_d$:

$$A_{dr} = \begin{cases} C\sqrt{V} & (V < V_d) \\ A_{dr}^{max} & (V > V_d) \end{cases} \quad (10)$$

where C is a proportional constant.

Fig. 4 well illustrates the point made above. In addition to the amplitude increase of the fast component with applied bias and saturation towards the full amplitude of the charge pulse, the time constant of the slow component has been observed to decrease with the bias, in agreement with eq. (5).

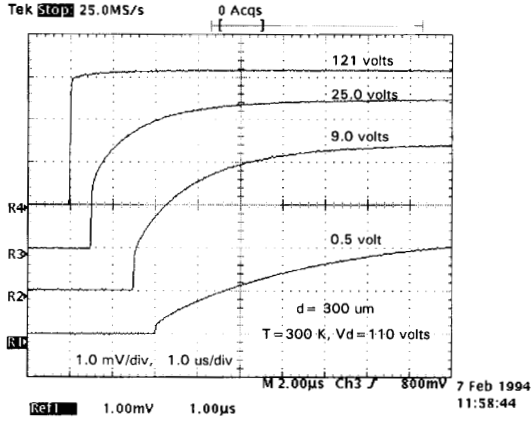


Fig. 4 Charge shapes for an irradiated detector ($\Phi_n = 3.29 \times 10^{13} \text{ n/cm}^2$) at RT with different operating biases. Laser illumination was on the n^+ side of the detector.

Fig. 5 shows the measured A_{dr} for the same detector shown in Fig. 4 as a function of $V^{1/2}$. The extrapolation of the linear part into the saturation gives the full depletion value $V_d = 110$ volts, which in turn gives the value of $N_{eff} = 1.60 \times 10^{12} \text{ /cm}^2$ using eq.(2) with $w = d$.

The charge shapes for the same detector shown in Fig.4 and 5, operated at a given bias but at various temperatures are shown in Fig. 6. It is clear that the time constant of the slow component τ_2 decreases drastically with the temperature. In fact, for a given bias, τ_2 depends on the temperature T through n or p :

$$\tau_2 \propto \begin{cases} e^{\frac{E_C - E_f}{kT}} & (\text{n-type}) \\ e^{\frac{E_f - E_V}{kT}} & (\text{p-type}) \end{cases} \equiv e^{\frac{E_F}{kT}} \quad (11)$$

($E_F = E_C - E_f$ or $E_f - E_V$)

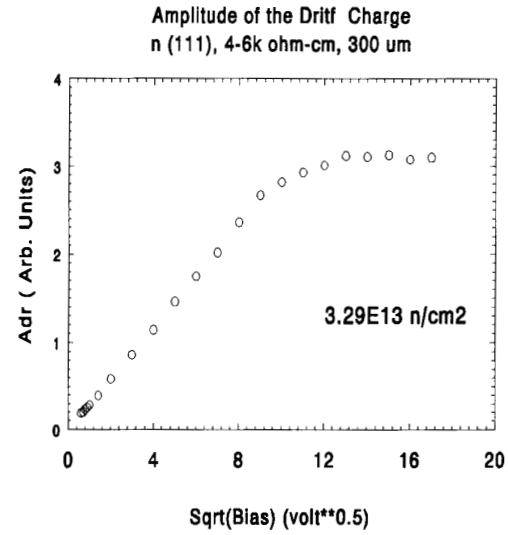


Fig. 5 Amplitude of the fast component (A_{dr}) in the charge shape as a function of the square root of the bias for an irradiated detector ($\Phi_n = 3.29 \times 10^{13} \text{ n/cm}^2$). A_{dr} saturates at the full depletion.

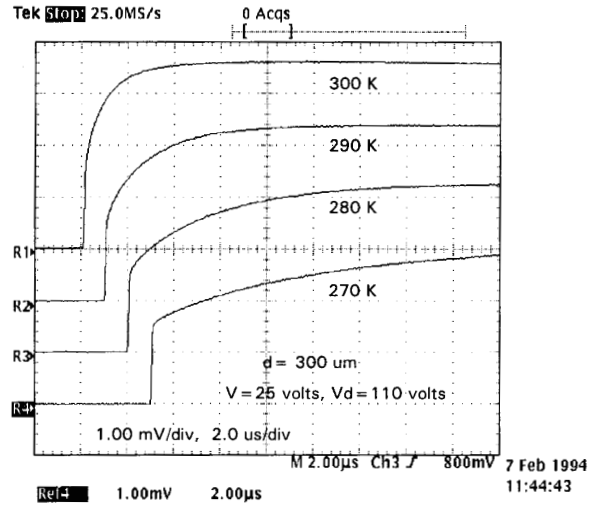


Fig. 6 Charge shapes for an irradiated detector ($\Phi_n = 3.29 \times 10^{13} \text{ n/cm}^2$) operated at a given bias at various temperatures. Laser illumination was on the n^+ side of the detector.

With a set of charge shapes shown in Fig. 6, one can make Arrhenius plots of τ_2 to obtain the values of the Fermi level. Fig. 7 shows such plots for detectors irradiated to $3.2 \times 10^{13} \text{ n/cm}^2$ and $5.89 \times 10^{14} \text{ n/cm}^2$. The extracted Fermi level positions are $E_F = 0.48 \text{ eV}$ and $E_F = 0.50 \text{ eV}$, respectively.

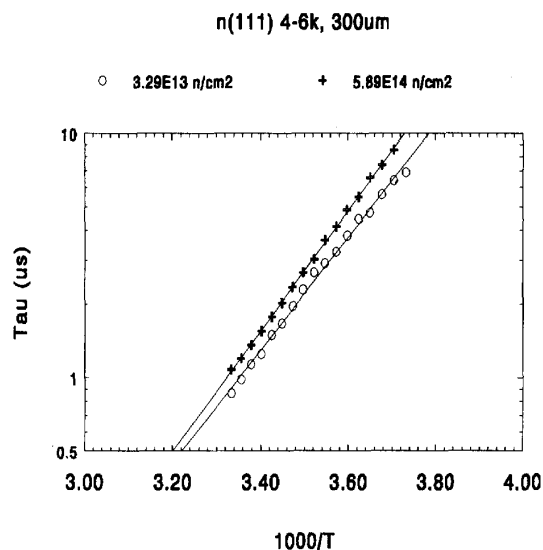


Fig. 7 Arrhenius plots of τ_2 for two detectors irradiated to different fluences.

It is necessary to say some words about the reproducibility of the TChT technique for obtaining the value of the Fermi level. Fig. 8 shows four Arrhenius plots for the detector #439-79 irradiated to 3.2×10^{13} n/cm². Each curve corresponds to a different bias or different thermal conditions (temperature sweeping up or down). Table I summarized the values of Fermi levels such obtained, which gives an estimation of accuracy of about 3% ($E_F = 0.50 \pm 0.02$ eV).

Table I Fermi level values obtained from various runs

V (V)	40	100	100	150	Ave.
T going	down	down	up	down	
E_F (eV)	0.51	0.49	0.51	0.48	0.50
Error (eV)				$\sigma =$	0.02

As shown in Fig. 9, the Fermi level is stabilized near the middle of the gap at all neutron fluences under study ($\Phi_n > 3.0 \times 10^{13}$ n/cm²), similar to the findings in ref.[10]. The clearly observed Fermi level stabilization near the middle of the band gap may be explained by the following considerations: 1) neutron radiation creates both acceptor and donor defect levels in the band gap. As the neutron fluence increases, the Fermi level would become independent on the original shallow impurity levels and be controlled by the spectrum of deep levels which are as a whole almost compensating; and 2) all these deep levels are distributed around the middle of the band gap, which would pin the Fermi level there.

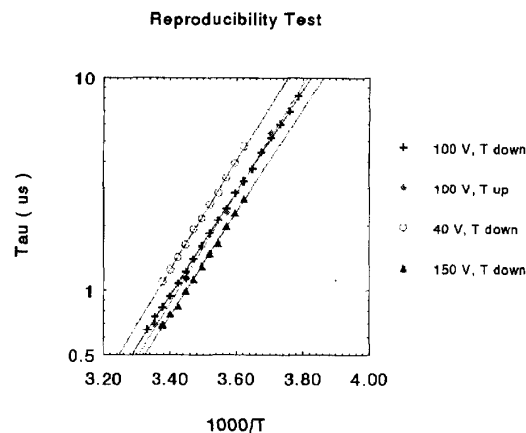


Fig. 8 Arrhenius plots of τ obtained from various runs.

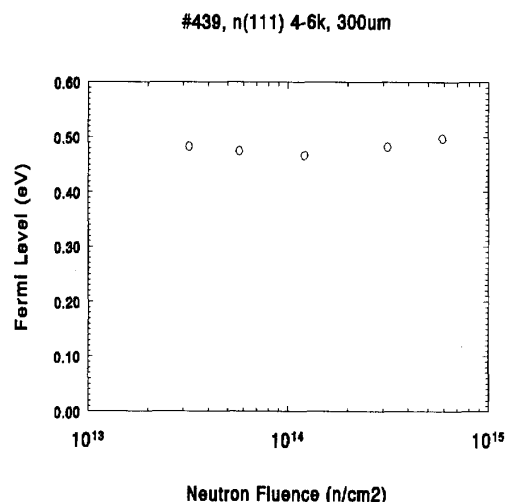


Fig. 9 Dependence of the Fermi level position on the neutron fluence.

IV. SUMMARY

It has been demonstrated in this paper that the TCT/TChT techniques are good alternatives to the traditional C-V methods, especially for highly irradiated, highly compensated materials and/or devices such as neutron damaged high resistivity silicon detectors. For the study of the ENB properties, the TChT technique is particularly powerful due its simplicities in sample preparation (no ohmic contact problem to the high resistivity substrate) and physical interpretation of the data.

The data presented in this paper are only an initial part of the study that will cover a wide range of neutron fluence. The high fluence data discussed in this work are of practical interest to the application of silicon detectors in the

high radiation environment in the proposed new Large Hadron Collider. The investigation of the Fermi level position changes at low fluences and fluences around the SCR inversion (the sign change of N_{eff}) point is of interest from a physical point of view and will be published elsewhere.

*This research was supported in part by the U.S. Department of Energy:

Contract No. DE-AC02-76CH00016, and by the National Research Council, Grant # LI-CAST93

ACKNOWLEDGMENTS

The authors would like to thank H.W. Kraner, T. Tsang, and S. Rescia of BNL for helpful discussions and comments to the improvement of the TCT/TChT system.

V. REFERENCES

- 1 G. Lindström, M. Benkert, E. Fretwurst, T. Schulz and R. Wunstorf, Proc. of the First International Conf. on Calorimetry in High Energy Physics, D.F. Anderson, et al., Des, (Word Scientific Publishing Co., Singapore, (1991) 467.
- 2 Z. Li, W. Chen, and H.W. Kraner, Nucl. Instr. and Meth. A308 (1991) 585.
- 3 Z. Li, "Modeling of the Frequency Dependent Characteristics of Neutron Irradiated p⁺-n Silicon Detectors After the Type Inversion in the Space Charge Region," BNL-49058, IEEE Nuclear Science Symposium, San Francisco, CA, (1993); accepted for publication in the IEEE Trans. Nucl. Sci. (in press).
- 4 R. Wunstorf, M. Benkert, N. Claussen, N. Croitoru, E. Fretwurst, G. Lindstrom, and T. Schulz, "Results on Radiation Hardness of Silicon Detectors up to Neutron Fluence of 10¹⁵ n/cm²", Nucl. Instr. Meths., A315, 149 (1992)
5. K. Gill, G. Hall, S. Roe, S. Sotthibandhu, R. Wheadon, P. Giubellino, and L. Ramello, "Radiation Damage by Neutrons and Photons to Silicon Detectors", Nucl. Instr. Meths., A322, 177 (1992).
- 6 H.W. Kraner, Z. Li, and E. Fretwurst, "The use of the Signal Current Pulse Shape to Study the Internal Electrical Field Profile and Trapping effects in Neutron Damaged Silicon Detectors", Presented at the Sixth European Symposium on Semiconductor Detectors, Milano, Italy, Feb. 24-26, 1992, Nucl. Instr. and Meth., A326 (1993) 350-356.
- 7 Z. Li, V. Eremin, N. Strokan, and E. Verbitskaya, "Investigation of the Type Inversion Phenomena: Resistivity and Carrier Mobility in the Space Charge Region and Electrical Neutral Bulk in Neutron Irradiated Silicon p⁺-n Junction Detectors", Presented at the IEEE Nucl. Sci. Symp, Orlando, FL, Oct. 25-31, 1992, Trans. Nucl. Sci. Vol. 40, No.4, 367(1993)
- 8 I. Tsvybak, B. Bugg, J. Walter, and J.A. Harvey, "Fast Neutron-Induced Changes in Net Impurity Concentration of High Resistivity Silicon", Trans. Nucl. Sci., Vol. 39, No.6, 1720(1992).
- 9 Z. Li, "Resistivity Measurements on Neutron Irradiated Detector Grade Silicon Materials", Presented at the 1st International Conference on Large Scale Application and Radiation Hardness of Semiconductor Detectors, Florence, Italy, July 7-9, 1993, to be published in Nuov Cimento (in press).
- 10 P.F. Lugakov, T.A. Lukashevich, and V.V Shussha, Phys. Sta. Sol., A, Vol. 74, 445(1982).
- 11 U. Biggeri, E. Borch, M. Bruzzi, S. Lazanu, Z. Li, and R. Beuttenmuller, "Type Inversion Measurements on Irradiated Silicon by Means of Hall Effect", Presented at the 1st International Conference on Large Scale Application and Radiation Hardness of Semiconductor Detectors, Florence, Italy, July 7-9, 1993, to be published in Nuov Cimento (in press).
- 12 V. Eremin, N. Strokan, E. Verbitskaya, and Z. Li, "The development of Transient Current and Charge Techniques for the Measurement of Effective Impurity Concentration in the Space Charge Region of p-n Junction Detectors," sub. to Nucl. Intrs. & Meth., (1994), BNL-60156.
- 13 V. Eremin, N. Strokan, and N. Tisnek, Sov. Phys. Semicond., Vol. 8, 1157(1974).
- 14 Z. Li and H.W. Kraner; "Modeling and Simulation of Charge Collection Properties For Neutron Irradiated Silicon Detectors"; BNL-48067; Presented at the 3rd International Conference on Advanced Technology and Particle Physics, Como, Italy, 22-26 June 1992; Nucl. Phys. B, Vol. 32, 398-409 (1993).